J BONE ONCOL 46 (2024) 100605

Contents lists available at ScienceDirect

Journal of Bone Oncology

journal homepage: www.elsevier.com/locate/jbo

Research Paper

FBXO22 is a potential therapeutic target for recurrent chondrosarcoma

Baoquan Xin [a,b,1], Hui Chen [c,1], Zhi Zhu [d,1], Qiujing Guan [e,1], Guangjian Bai [a,b], Cheng Yang [a], WeiWei Zou [f], Xin Gao [a,*], Lei Li [c,e,*], Tielong Liu [a,*]

[a] Department of Orthopaedic Oncology, Changzheng Hospital, Navy Medical University, No. 415 Fengyang Road, Shanghai, 200003, China
[b] School of Health Science and Engineering, University of Shanghai for Science and Technology, Shanghai, 200003, China
[c] Joint Center for Translational Medicine, Shanghai Fifth People's Hospital, Fudan University and School of Life Science, East China Normal University, Shanghai, 200241, China
[d] Department of Pathology, Changzheng Hospital, Navy Medical University, No. 415 Fengyang Road, Shanghai, 200003, China
[e] Shanghai Key Laboratory of Regulatory Biology, Institute of Biomedical Sciences, School of Life Sciences, East China Normal University, 500 Dongchuan Road, Shanghai 200241, China
[f] Department of Medical Imaging, Changzheng Hospital, Navy Medical University, No. 415 Fengyang Road, Shanghai, 200003, China

HIGHLIGHTS

- FBXO22 is dramatically highly expressed in clinical samples of recurrent chondrosarcoma.
- FBXO22 is prominently upregulation in cell line-derived xenograft samples of recurrent chondrosarcoma and in recurrent chondrosarcoma cells.
- Suppressing FBXO22 abates the proliferation and migration of recurrent chondrosarcoma cells.
- Suppressing FBXO22 facilitates the apoptosis of recurrent chondrosarcoma cells.
- Suppressing FBXO22 raises the expression of PD-L1 in recurrent chondrosarcoma.

ARTICLE INFO

Keywords:
Bone tumor
Chondrosarcoma
Recurrence
PD-L1
Therapeutic target

ABSTRACT

Chondrosarcoma (CHS) is a malignant bone tumor with insensitivity to both radiotherapy and chemotherapy, and a high recurrence rate. However, the latent mechanism of recurrent CHS (Re-CHS) remains elusive. Here, we discovered that FBXO22 was highly expressed in clinical samples of Re-CHS. FBXO22 played a significant role in various cancers. However, the role of FBXO22 in Re-CHS remained unclear. Our research demonstrated that suppressing FBXO22 abated the proliferation and migration of CHS cells and facilitated their apoptosis. In addition, suppressing FBXO22 raised the expression of PD-L1 in Re-CHS. All these findings provide new evidence for using FBXO22 and PD-L1 as combined targets to prevent and treat Re-CHS, which may prove to be a novel strategy for immunotherapy of CHS, especially Re-CHS.

1. Introduction

Chondrosarcoma (CHS) is the second most common primary malignant bone tumor, with an overall incidence of about 1 in 200,000, accounting for 9.2 % of all primary malignant bone tumors. The mean age of onset is around 50 years, with male preference [1,2]. The prognosis of CHS is closely related to its histological grade. The 5-year survival rate for grade 1, 2 and 3 CHS is 90 %, 81 % and 29 % respectively. The recurrence rate of CHS increases with the severity of the malignancy grade, an about 50 % recurrence rate for low-grade CHS and 78 % for intermediate-grade CHS [3–6]. In addition, CHS tends to progress to higher grades upon recurrence [7].

Surgical excision remains the mainstay of treatment for CHS at present. But even with complete removal of the CHS tissue, the recurrence rate for medium-grade CHS remains high as 50 %. When complete excision is difficult due to complex anatomical structures, the recurrence rate can exceed 85 % [3]. In addition to surgical treatment, CHS is insensitive to radiation and chemotherapy, highlighting the urgent need for a new therapeutic approach to effectively control the disease [8,9]. Immunotherapy, as a novel treatment approach in recent years, has

* Corresponding authors.
E-mail addresses: 15026962975@163.com (X. Gao), lllkzj@163.com (L. Li), czyygzl@163.com (T. Liu).
[1] These authors contributed equally to this study and should be considered as co-first authors.

https://doi.org/10.1016/j.jbo.2024.100605
Received 2 January 2024; Received in revised form 27 March 2024; Accepted 30 April 2024
Available online 1 May 2024

shown promising results in many cancers. However, research on immunotherapy of CHS is still in the infant stage [10–12]. According to analyses of a small number of cases, some CHS patients have been shown to benefit from PD-1 antibody treatment [13–15].

F-box proteins are components of E3 ubiquitin ligase complexes, and FBXO22 is a member of the F-box protein family. It has been identified to play a notable role in the development and progression of cancers such as liver cancer, colorectal cancer, breast cancer, and lung cancer [16–19]. An analysis of TCGA data showed that the mRNA level of FBXO22 was significantly elevated in various types of human tumor tissues compared to normal tissues [20]. The expression of PD-L1 has been shown to be regulated by various factors, among which FBXO22 could degrade PD-L1 through the ubiquitination pathway [21,22]. However, the biological function of FBXO22 in recurrent CHS (Re-CHS) and its potential relationship with PD-L1 in CHS are still not fully understood.

In this study, we investigated the impact of FBXO22 on the occurrence and progression of Re-CHS, as well as its potential relationship with PD-L1 in the treatment of CHS. We demonstrated that FBXO22 could expedite the proliferation and migration of Re-CHS cells and attenuate their apoptosis. Most notably, PD-L1was found to be upregulated in Re-CHS by downregulating the level of FBXO22, which may provide a novel strategy for immunotherapy of Re-CHS.

2. Results

2.1. FBXO22 is highly expressed in clinical Re-CHS samples

To investigate the molecular mechanism underlying the recurrence of CHS, we collected primary CHS (Pr-CHS) and Re-CHS paraffin section samples from the same patient (n = 3) and performed mass spectrometry analysis (Fig. 1**A**). In the proteomic analysis results, we referenced literature related to protein expression studies [23–29], using a fold change greater than 1.2 or less than 0.83 as the selection criteria for differential protein genes. A total of 166 differentially expressed (DE) proteins were identified, including 117 upregulated proteins and 49 downregulated proteins (FC > 1.2 or FC < 0.83, P < 0.05) (Fig. 1**B**). Later, we focused on DE proteins with P value less than 0.01 (Fig. 1**C**), and validated the mRNA expression of top 15 upregulated candidates in the re-collected fresh Pr-CHS and Re-CHS samples from the same patient (n = 3) by qRT-PCR assay. It was found that the mRNA levels of *FBXO22*, *MACROH2A* and *PRPF19* were highly expressed (Fig. 1**D**), among which *FBXO22* played a notable role in the development and progression of cancers such as liver cancer, colorectal cancer, breast cancer, and lung cancer [16–19]. However, the role of FBXO22 in Re-CHS remained unclear. Subsequently, we utilized IHC and Western blot assay to further validate the expression of FBXO22 in clinical Pr-CHS and Re-CHS tissues (Fig. 1**E-H**), and found that the FBXO22 protein expression was significantly upregulated in clinical Re-CHS tissues.

2.2. FBXO22 is prominently upregulated in cell line-derived xenograft (CDX) samples of Re-CHS cells

To further explore the function of FBXO22 in Re-CHS, we established a CDX mouse model of Re-CHS using CHS cell line (HCS2/8 cell or SW1353 cell) (Fig. 2**A**), from which CDX cells were isolated (Fig. S1**A**). Pr-CHS and Re-CHS tissues were collected in CDX mouse models for IHC validation (Fig. 2**B and S1B**). The results indicated that the expression of FBXO22 in Re-CHS tissues was significantly higher than that in Pr-CHS tissues from the CDX mouse model. Further Western blot and qRT-PCR assays showed that the FBXO22 expression in Re-CHS tissues and cells from the CDX mouse model was upregulated significantly (Fig. 2**C, D and S1C, D**). In the Re-CHS CDX mouse model, the Re-CHS tumors grow faster and have a larger volume than the Pr-CHS tumors. This may lead to a hypoxic environment for Re-CHS cells. Therefore, to exclude the potential effects of hypoxia, we examined the protein level of FBXO22 in Pr-CHS and Re-CHS cells with different degrees of confluence. The results showed that the protein level of FBXO22 did not change under different fusion degrees **(**Fig. S1**E).** Based on these findings, we hypothesized that FBXO22 might indeed be a relevant gene associated with CHS recurrence.

2.3. FBXO22 accelerates proliferation of Re-CHS in vivo and in vitro

To clarify the role of FBXO22 in Re-CHS, we established the Re-CHS cell lines Re-HCS2/8 and Re-SW1353 using Re-CHS CDX samples. Employing lentiviral-mediated shRNA infection, we separately generated stable cell lines with FBXO22 knockdown in Re-CHS cell lines, using shN as the negative control (Fig. 3**A and S2A**). We selected Re-HCS2/8 shFBXO22 #2 and Re-SW1353 shFBXO22 #1 as experimental cells due to their higher knockdown efficiency within Re-HCS2/8 and Re-SW1353 cells. To investigate the impact of FBXO22 on the viability of CHS cells, we conducted cell viability assays using the Cell Counting Kit-8 (CCK-8) on Re-HCS2/8 shN and shFBXO22 #2 cells and found that knocking down FBXO22 significantly decreased the cell viability of Re-HCS2/8 cells (Fig. 3**B**). The colony formation assay demonstrated a significant reduction in colony formation upon FBXO22 knockdown in both Re-HCS2/8 (Fig. 3**C, D**) and Re-SW1353 ($p < 0.0001$, Student's *t*-test) cells **(**Fig. S2**B, C**). To explore whether FBXO22 knockdown enhanced the growth of Re-CHS cells in vivo, we subcutaneously injected stably FBXO22-downregulated Re-HCS2/8 shFBXO22 #2 cells and controlled Re-HCS2/8 shN cells into the inguinal region of 5-week-old nude mice. When the primary tumors reached a size of 500 mm^3, more than 95 % were excised. Eight days later, the recurrent tumors were removed for measurement. Consistent with the in vitro results, the volume and weight of recurrent tumors in the FBXO22 knockdown group were significantly lower than those in the control group **(**Fig. 3**E, F, G).** We also designed a control experiment using the same tumor-bearing method to compare the growth rates of primary tumors in both groups. The results showed that, consistent with the in vitro results, the growth rate of Re-HCS2/8 shFBXO22 #2 tumors subcutaneously implanted in mice was notably slower than that carrying the empty vector (Fig. 3**H**). The tumor volume and weight were significantly lower in FBXO22 knockdown group than that in the control group on day 18 (Fig. 3**I, J**). Interestingly, we observed a significant difference in the body weight of the two groups of mice as the tumors grew (Fig. S2**D**). These findings collectively indicate that FBXO22 could promote the growth of Re-CHS both in vitro and in vivo.

2.4. FBXO22 promotes the migration and abates apoptosis of Re-CHS cells in vitro

It is reported in the literature that the malignant grade of CHS will increase with recurrence [7], and the metastasis rate will also increase sharply with the increase of malignancy [3]. To further investigate the effect of FBXO22 on metastasis and malignancy in Re-CHS, cell migration and apoptosis were detected in the Re-CHS cell lines Re-HCS2/8 and Re-SW1353. Scratch assay results revealed that FBXO22 knockdown significantly decelerated the migration rate of Re-HCS2/8 (Fig. 4**A, B**) and Re-SW1353 (Fig. 4**C, D**) cells. Flow cytometry analysis of apoptosis showed a pronounced increase in apoptotic levels for both Re-HCS2/8 (Fig. 4**E, F**) and Re-SW1353 (Fig. 4**G, H**) upon FBXO22 knockdown. In summary, these results suggest that FBXO22 also played a role in promoting the migration of Re-CHS cells and inhibiting the apoptosis during the process of CHS recurrence.

2.5. FBXO22 downregulates the expression of PD-L1 in Re-CHS

Previous studies reported that FBXO22 downregulated the expression of PD-L1 in lung cancer cells [21,22]. To further investigate the potential role of FBXO22 in the treatment of CHS, we examined the expression relationship between F BXO22 and PD-L1 in CHS at both the

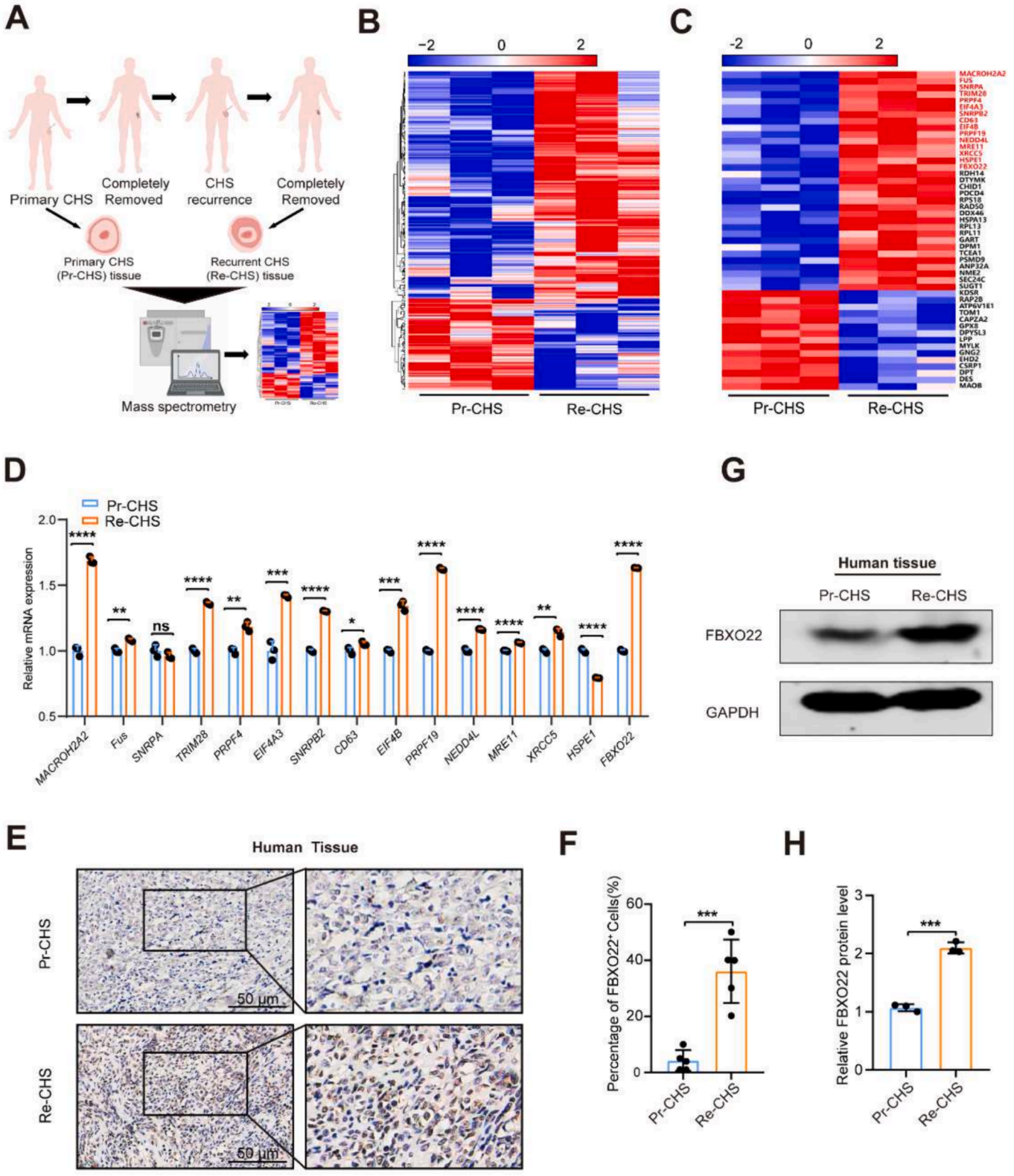

Fig. 1. FBXO22 is highly expressed in clinical samples of Re-CHS patients. **A** Schematic illustration of the analysis by mass spectrometry analysis of Pr-CHS and Re-CHS samples from the same patient (created by Biorender); **B** Mass spectrometry analysis identified differential proteins (FC > 1.2 or FC < 0.83, P < 0.05) (n = 3); **C** A Volcano blot showing differential expression (DE) proteins (FC > 1.2 or FC < 0.83, P < 0.01) and top 15 upregulated proteins; **D** The mRNA levels of the top 15 upregulated candidates were detected in Pr-CHS and Re-CHS tissues from patients by qRT–PCR (n = 3); **E** Representative images of FBXO22 IHC staining in Pr-CHS and Re-CHS tissues (n = 5); **F** Quantification of FBXO22^{+} signals from E; **G** Western blot detection of the protein expression levels of FBXO22 in Pr-CHS and Re-CHS tissues from patients (n = 3). GAPDH was used as a control; **H** Quantification of signals from G.

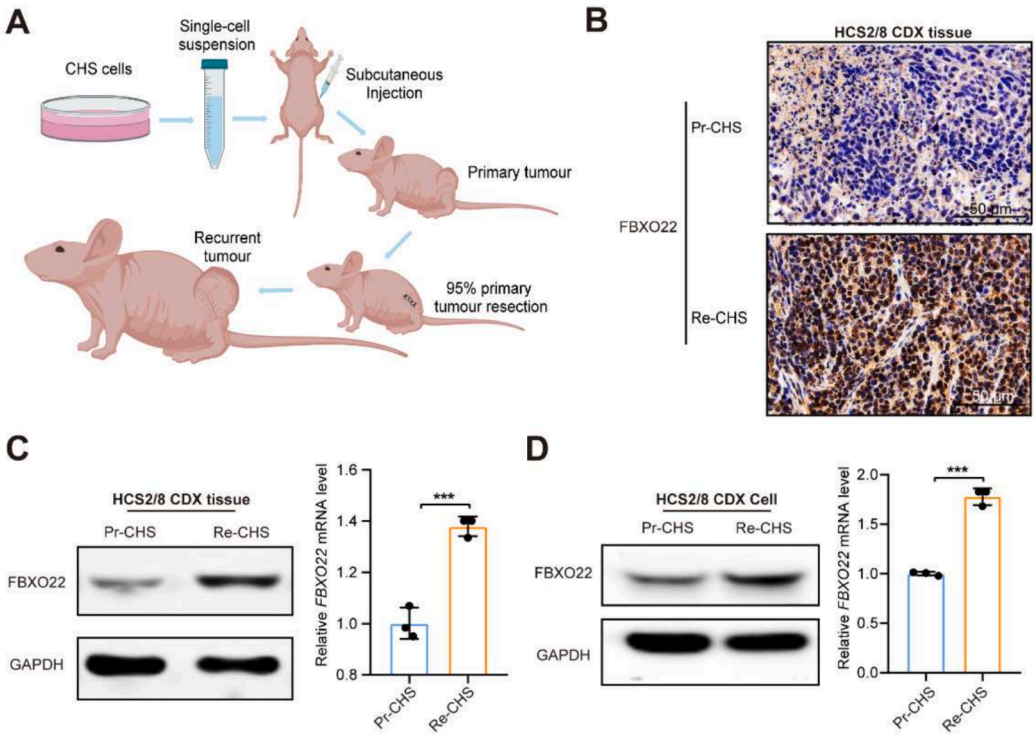

Fig. 2. FBXO22 is prominently upregulated in cell line-derived xenograft (CDX) samples of Re-CHS and in Re-CHS cells. A Schematic illustration of the Re-CHS CDX model in nude mice; **B** Representative images of FBXO22 IHC staining in Pr-CHS and Re-CHS tissues from the CDX model of HCS2/8 cells (n = 5); **C** Left, Western blot detection of the protein expression level of FBXO22 in Pr-CHS and Re-CHS tissues from CDX model of HCS2/8 cells (n = 3). GAPDH was used as a control. Right, qRT-PCR detection of the mRNA level of *FBXO22* in Pr-CHS and Re-CHS tissues from CDX model of HCS2/8 cells (n = 3); **D** Left, Western blot detection of the protein expression level of FBXO22 in Pr-CHS and Re-CHS cells from CDX model of HCS2/8 cells (n = 3). GAPDH was used as a control. Right, qRT-PCR detection of the mRNA level of *FBXO22* in Pr-CHS and Re-CHS cells from CDX model of HCS2/8 cells (n = 3).

cellular and tissue levels. Consistent with previous research findings, we discovered that FBXO22 and PD-L1 expression levels exhibited an inverse trend in human CHS tissue samples. In human Pr-CHS tissue sections, FBXO22 expression was lower, while PD-L1 exhibited higher expression in corresponding locations. In tissue sections from Re-CHS, FBXO22 expression was elevated, and correspondingly, PD-L1 expression was decreased (Fig. 5**A**). Subsequently, we conducted an analysis on the protein level of Re-HCS2/8 shFBXO22 #2 and Re-SW1353 shFBXO22 #1 cells with FBXO22 knockdown (Fig. 5**B**), and found that when FBXO22 was knocked down, the PD-L1 expression rebounded. We further analyzed the tumor tissues from the mice bearing tumors as shown in Fig. 3**H**, and the results were consistent with the cellular findings. FBXO22 and PD-L1 exhibited a negative correlation at the protein (Fig. 5**C**) and tissue slice levels (Fig. 5**E**). We also measured the protein level of CDK5 in CHS cells, and the results were consistent with the regulatory mechanism reported in lung cancer cells. The trend of CDK5 protein expression change was consistent with PD-L1 and opposite to FBXO22. The protein level of CDK5 was higher in Pr-CHS cells than in Re-CHS cells **(**Fig. 5**D)**. To rule out any potential effect of the tumorigenic process in nude mice on CHS cells, we silenced FBXO22 in untreated CHS cell line HCS2/8 using siRNA, creating HCS2/8 siFBXO22, using HCS2/8 siN as negative controls. The result showed that lowering the expression of FBXO22 in the original cell lines induced the upregulation of PD-L1 protein (Fig. S3**A**). All these findings demonstrated that FBXO22 downregulated PD-L1 expression in Re-CHS.

3. Discussion

The recurrence of CHS severely impacts the patients' quality of life and survival time [5], creating a significant burden on both their families and society. Through clinical samples of Pr-CHS and Re-CHS, we discovered that FBXO22 was a critical regulatory factor in malignant progression of Re-CHS (Fig. 6). In addition, FBXO22 was found to be closely correlated with the immune checkpoint PD-L1 within CHS, which is the first study from the perspective of recurrence to investigate the malignant biological behavior and targeted treatment of CHS.

An increasing number of studies have demonstrated the crucial role of FBXO22 in carcinogenesis. Multiple studies have revealed that in breast cancer, FBXO22 could regulate the KDM4 protein family and participated in the development, differentiation, and tamoxifen resistance of breast cancer [30,31]. Interestingly, FBXO22 exhibited different functions in the occurrence and metastasis of breast cancer, while promoting breast cancer. Zhang et al. [16] and Tian et al. [32] reported that FBXO22 promoted tumor proliferation and invasion in liver cancer. It could also regulate the expression levels of P21 and Krüppel-like factor 4 (KLF4) through the ubiquitination pathway, thus affecting the cell cycle. In lung cancer, colorectal cancer, and melanoma, FBXO22 also played a significant role in tumor occurrence and invasion. Studies indicate that FBXO22 further promoted tumor occurrence and metastasis by degrading different substrates in these tumors [17,19,33]. By validating samples from both patients and nude mice, including Pr-CHS and Re-CHS samples, we discovered that the FBXO22 expression level in Re-CHS was significantly higher than that in Pr-CHS samples. This finding led us to the speculation that FBXO22 might be closely associated with CHS recurrence. To confirm the role of FBXO22 in the development of CHS, we engineered a Re-CHS cell line with reduced FBXO22 expression and established a mouse model of Re-CHS. The results indicate that the downregulation of FBXO22 suppressed cell proliferation and migration, but promoting cell apoptosis. These findings suggest that FBXO22 plays an oncogenic role in CHS.

In addition to playing a critical role in the occurrence and progression of tumors, FBXO22, as part of the E3 ubiquitin ligase complex, may

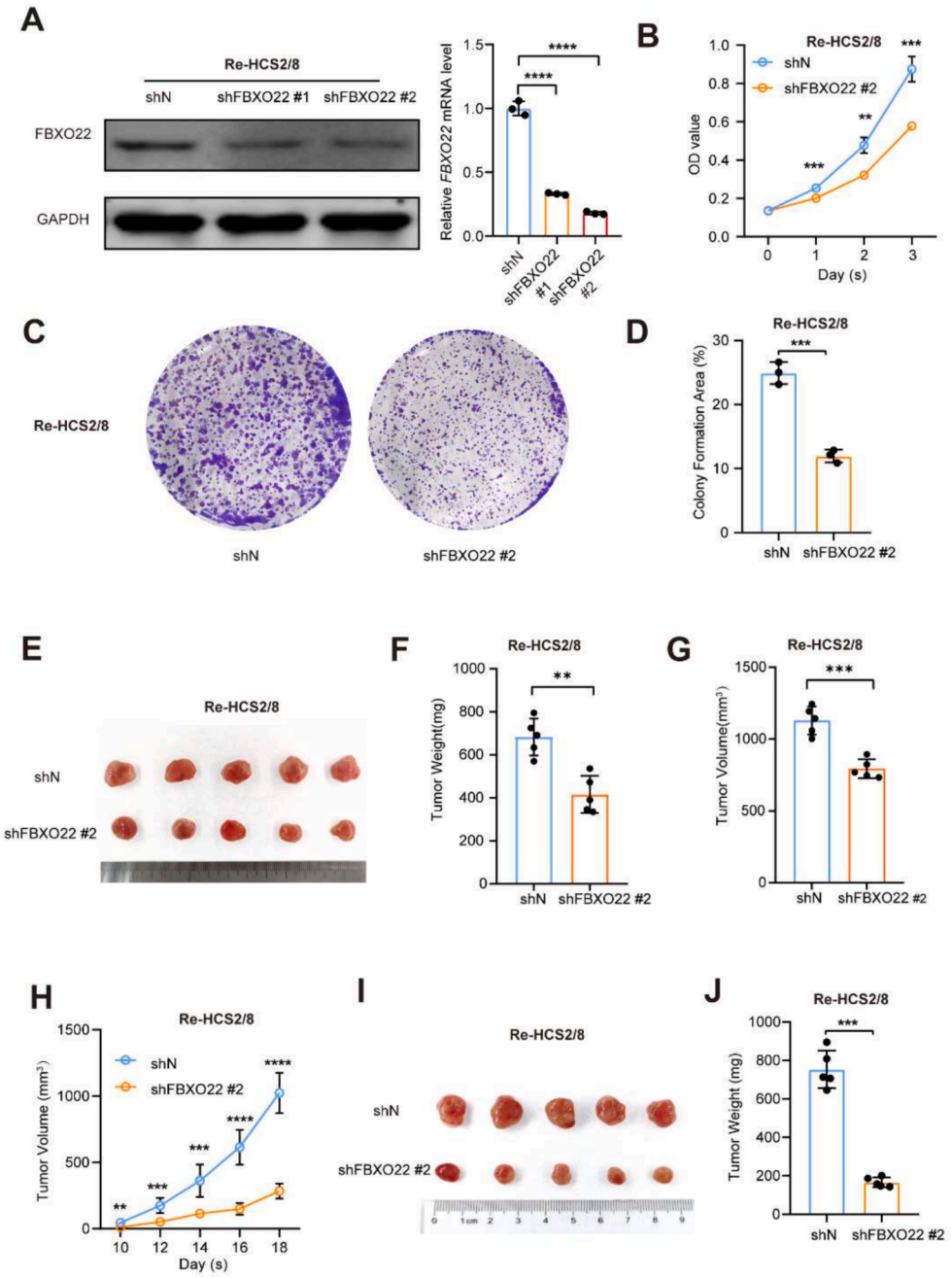

Fig. 3. FBXO22 accelerates proliferation of Re-CHS in vivo and in vitro. A Left, western blot detection of the protein expression level of FBXO22 in Re-HCS2/8 shN, shFBXO22 #1 and shFBXO22 #2 cells. Right, qRT-PCR detection of the mRNA level of *FBXO22* in Re-CHS shN, shFBXO22 #1 and shFBXO22 #2 cells; **B** Re-HCS2/8 shN and shFBXO22 #2 cells were subjected to Cell Counting Kit-8 (CCK-8) assay to detect cell viability; **C** Re- HCS2/8 shN and shFBXO22 #2 cells were conducted to detect cell proliferative ability by colony formation assay; **D** Quantification of signals from C; **E, F, G** In vivo analysis of Re-CHS in mice that were subcutaneously injected with Re-HCS2/8 shN and Re-HCS2/8 shFBXO22 #2 cells. When the primary tumors reached a size of 500 mm^3, more than 95 % were excised. Eight days later, the recurrent tumors were removed and their weight and volume were recorded; **H** In vivo analysis of Re-CHS in mice that were subcutaneously injected with Re-HCS2/8 shN and and Re-HCS2/8 shFBXO22 #2 cells. Starting from day 10, the Re-HCS volume was measured; **I, J** In vivo analysis of Re-CHS in mice that were subcutaneously injected with Re-HCS2/8 shN and and Re-HCS2/8 shFBXO22 #2 cells. When the maximum Re-HCS volume reached 1000 mm^3, tumors were excised and their weight was recorded.

contribute to tumor therapy through the ubiquitination pathway, leading to the degradation of various substrate proteins associated with cancer treatment [18,34]. Research reports have shown that FBXO22 can degrade CD147, a protein associated with drug resistance in lung cancer, through the ubiquitination pathway, thereby enhancing the sensitivity of lung cancer cells to cisplatin [35]. It is well known that CHS is a tumor that is insensitive to both radiation and chemotherapy, and it is prone to recurrence. Its recurrence rate remains high despite efforts to achieve complete surgical resection, and its malignancy tends to increase with recurrence [3,7]. Research by Sarmishtha et al. indicates that FBXO22 can enhance the sensitivity of lung cancer cells to DNA damage therapy by downregulating PD-L1 [22]. Furthermore, studies have shown that some CHS patients benefited from treatment with PD-1 antibodies [13–15]. Therefore, it is speculated that FBXO22 and PD-L1 expression might also be correlated in CHS. IHC analysis of Re-CHS showed that as FBXO22 expression increased, PD-L1 expression

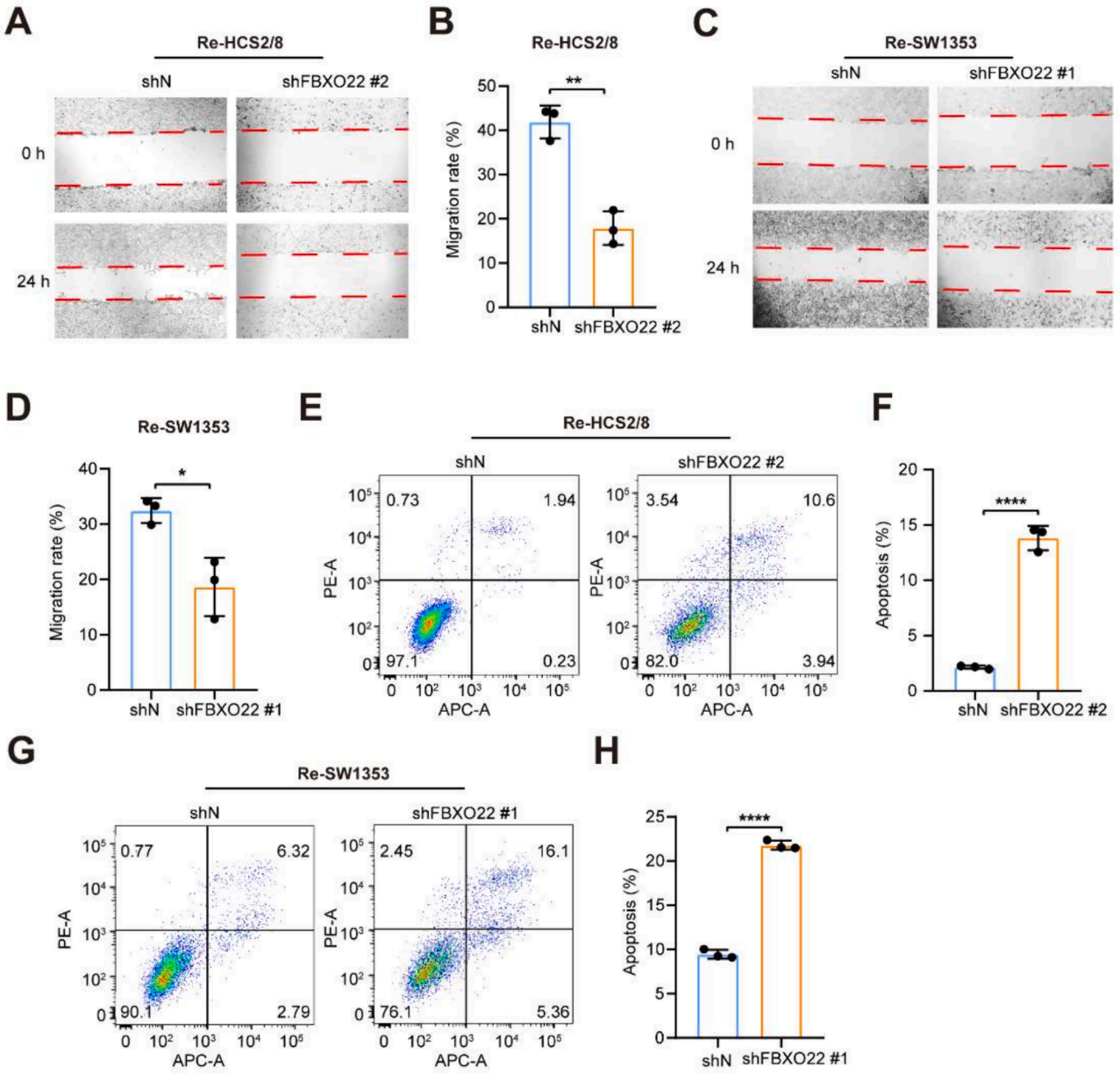

Fig. 4. FBXO22 promotes the migration of Re-CHS and abates apoptosis in vitro. A, B Re-HCS2/8 shN and shFBXO22 #2 cells were conducted to detect the cell migration ability by wound healing assay (A), cell migration rates of Re-HCS2/8 shN and shFBXO22 #2 cells were measured by ImageJ software(B); **C, D** Re-SW1353 shN and shFBXO22 #1 cells were conducted to detect the cell migration ability by wound healing assay **(C)**, cell migration rates of Re- SW1353 shN and shFBXO22 #1 cells were measured by ImageJ software **(D)**; **E, F** Re-HCS2/8 shN and shFBXO22 #2 cells were conducted to detect the cell apoptosis ability by flow cytometry using PI/APC apoptosis kit **(E)** and cell apoptosis rate **(F)**; **G, H** Re-SW1353 shN and shFBXO22 #1 cells were conducted to detect cell apoptosis ability **(G)** and cell apoptosis rate **(H)** by flow cytometry using PI/APC apoptosis kit.

decreased. When FBXO22 was downregulated in Re-CHS, PD-L1 expression increased. These findings suggest that FBXO22 could potentially serve as a combined therapeutic target with PD-L1 for Re-CHS.

Due to the difficulty in collecting paired samples of Pr-CHS and Re-CHS, the clinical sample size used in this study was relatively small. However, we successfully established a nude mouse model of Re-CHS and validated our hypothesis through animal experiments. It has been reported that inhibiting CDK5 could hinder the phosphorylation of FBXO22, thus increasing the FBXO22 expression and subsequently affecting the expression level of PD-L1 [22]. In our study, we found that the protein expression level of CDK5 in Pr-CHS cells was higher than that in Re-CHS cells. Moreover, the trend of CDK5 protein expression change was consistent with PD-L1 and opposite to FBXO22, which is in line with the relevant signaling mechanisms reported in lung cancer. These findings suggest that further in-depth research is warranted for comprehensive analysis and validation, and it might be possible to downregulate the oncogenic effect of FBXO22 indirectly or directly by enhancing the function of CDK5 or designing inhibitors for FBXO22. Simultaneously, upregulating PD-L1 could expose immune checkpoints, potentially enabling the use of combined PD-1 antibodies for treating Re-CHS. MiniPDX, an emerging method for rapidly testing the sensitivity of anticancer drugs, has gained increasing attention in recent years [36–38]. It reliably simulates patients' clinical treatment responses, which could become a reliable tool for conducting experimental treatments in our context.

Taken together, FBXO22 is highly expressed in Re-CHS. In vitro experiments have shown that FBXO22 can promote the proliferation and

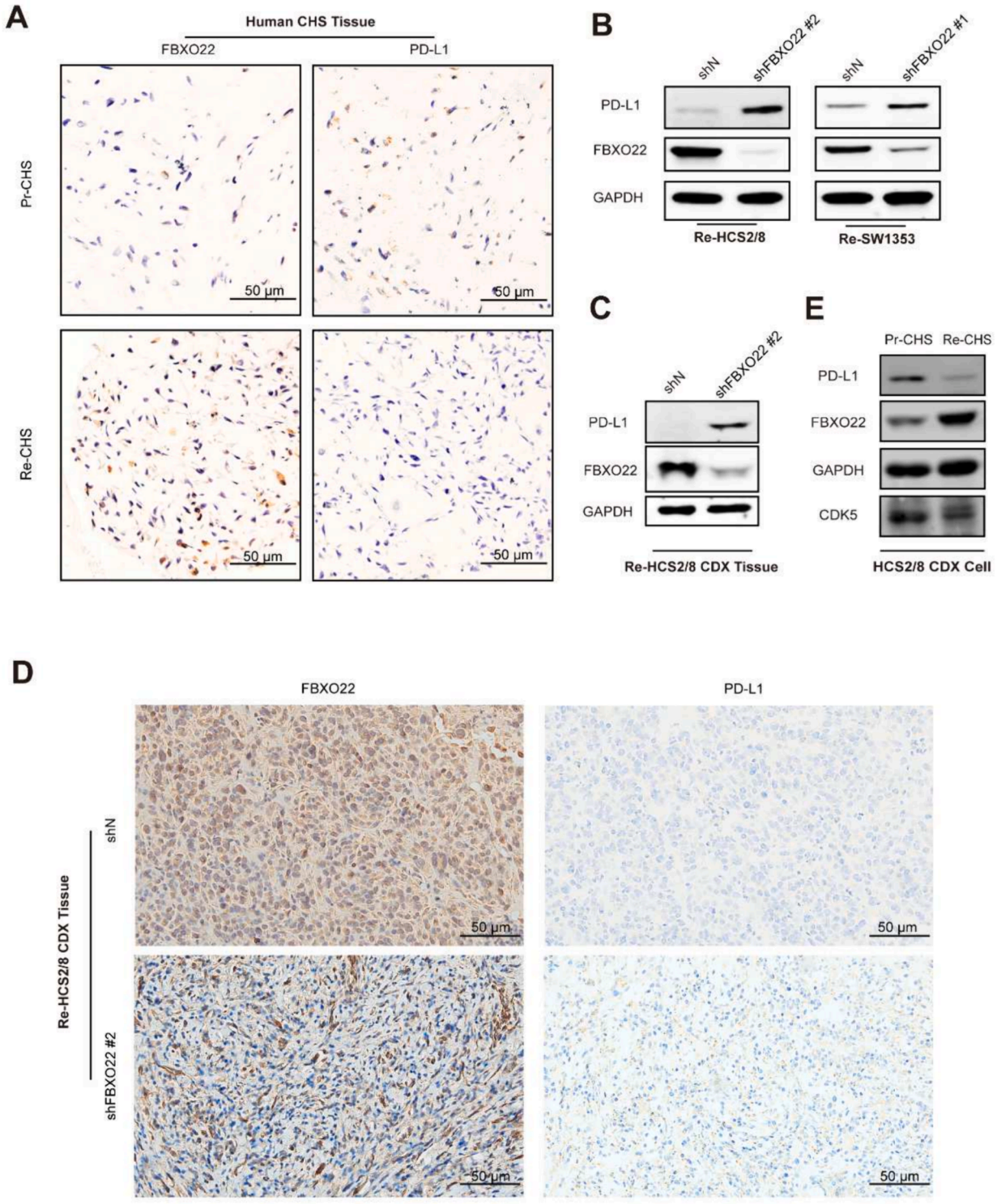

Fig. 5. FBXO22 downregulates the expression of PD-L1 in Re-CHS. A Representative images of FBXO22 and PD-L1 IHC staining in Pr-CHS and Re-CHS tissues; **B** Western blot detection of the protein expression level of FBXO22 and PD-L1 in Re-HCS2/8 shN, Re-HCS2/8 shFBXO22 #2, Re-SW1353 shN and Re-SW1353 shFBXO22 #1 cells; **C** Western blot detection of the protein expression level of FBXO22 and PD-L1 in Re-CHS tissues from the CDX model of Re-HCS2/8 shN and shFBXO22 #2 cells; **D** Representative images of FBXO22 and PD-L1 IHC staining in Re-CHS tissues from the CDX model of Re-HCS2/8 shN and shFBXO22 #2 cells; **E** Western blot detection of the protein expression level of CDK5, FBXO22, and PD-L1 in primary or recurrent HCS2/8 CDX cells.

migration of Re-CHS cells while inhibiting their apoptosis. Additionally, in vivo studies have demonstrated that FBXO22 can enhance the tissue growth of Re-CHS. FBXO22 downregulates PD-L1 in CHS, indicating its potential as a combined target for immunotherapy. Furthermore, this study presents the first report of the inhibitory effects of FBXO22 knockdown on Re-CHS and proposes the possibility of using FBXO22 as a therapeutic target in combination with PD-L1 for immunotherapy, offering a new avenue for targeted treatment of Re-CHS.

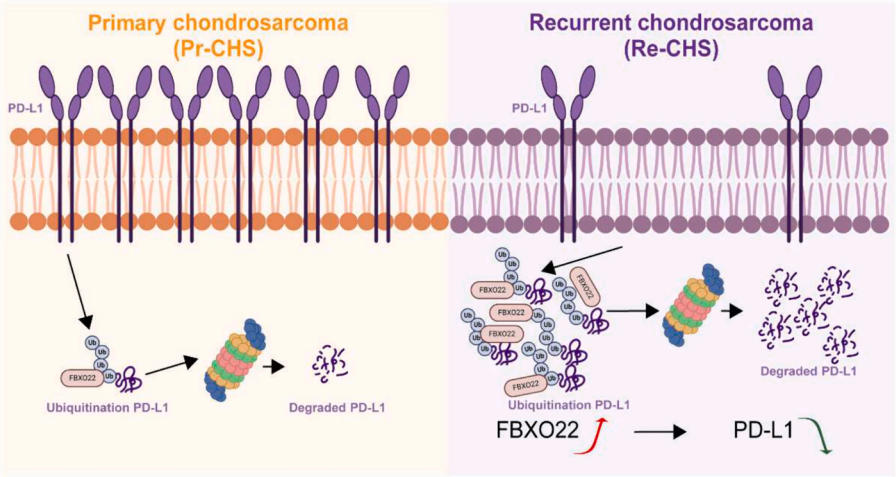

Fig. 6. A putative schematic presentation of FBXO22 regulating PD-L1 expression in recurrent chondrosarcoma. In Re-CHS, FBXO22 is upregulated, stimulating the growth of Re-CHS and enhancing the degradation of PD-L1.

4. Methods

4.1. Clinical samples and mass spectrometry analysis

Clinical Pr-CHS and Re-CHS samples were procured from the Department of Bone Tumors and Pathology at Changzheng Hospital (Shanghai, China). The research project received approval from the hospital's ethics committees, and all participating patients provided informed consent in accordance with state and institutional regulations governing the experimental use of human tissues. From the acquired clinical tumor samples, the Pr-CHS and Re-CHS samples from the same patient (n = 3) were selected. Protein mass spectrometry analysis was commissioned to Shanghai APTBIO Co. for thorough evaluation.

4.2. Animal study

We adapted the mouse tumor recurrence model construction methods to create a Re-CHS model in nude mice [39,40]. Thirty male nude mice (Shanghai Slac Laboratory Animal Co., Ltd., Shanghai, China) were raised in the specific pathogen-free (SPF) environment. By injecting 2×10^6 cells/100 μL of HCS2/8 (or SW1353) cells into the inguinal region of the male nude mice, we established the model, followed by housing the mice in SPF animal facilities. When the primary tumors reached a size of 500 mm^3, mice were anesthetized with 1 % pentobarbital sodium. Subsequently, more than 95 % of the primary tumor was removed, leaving less than 5 % of residual tumor tissue to simulate residual micro-tumors. In cases where the recurrent tumor grew to 1000 mm^3 or the body weight decreased by 15 % within one week, euthanasia was carried out, and the recurrent tumor was excised for further analysis.

We constructed a CDX mouse model using the Re-CHS cell line with FBXO22 knockdown. Male nude mice were subcutaneously injected with 2×10^6 cells/100 μL of Re-HCS2/8 shFBXO22 #2 and Re-HCS2/8 shN cells, respectively, into the inguinal region. The mice were then housed in SPF animal facilities. Starting from the 10th day post-injection, we measured the tumor size and recorded the weight of the mice. When the volume of the first tumor reached 1000 mm^3, euthanasia was carried out on both groups of mice, and the tumors were excised for further analysis. Animal care and experiments adhered to all ethical regulations related to animal research, as approved by the Committee for Humane Treatment of Animals at East China Normal University (Shanghai, China).

4.3. Cell lines and cell culture

The Re-CHS CDX tissues were aseptically dissected into 1 mm^3 fragments. These fragments were then added to 1 mL digestion solution consisting of 2 mg collagenase II (Sigma, C6885), 1 mL phosphate buffered saline (PBS), and 10 μL 1 M hepes, and were digested at 37 °C for 30 min. Following digestion, the cell suspension was obtained. Following centrifugation at 1500 rpm for 10 min, the supernatant was removed, and the cell pellet was reconstituted in Dulbecco's Modified Eagle's Medium (DMEM, C11995500BT) supplemented with 20 % fetal bovine serum (FBS) (Gibco, 10270–106), 100 U/mL of penicillin, and 100 mg/mL of streptomycin (Invitrogen, 15070063). The resuspended cells were plated in culture dishes and maintained at 37 °C with 5 % CO_2. After 24-h culture, the medium was replaced with full DMEM culture medium (10 % FBS, 100 U/L penicillin, and 100 mg/L streptomycin) for subculturing. This process resulted in the establishment of Re-CHS cell lines Re-HCS2/8 and Re-SW1353.

The human CHS cell line SW1353, and HCS-2/8 were procured from the American Type Culture Collection (ATCC, Manassas, Virginia, USA). Both cell lines were cultured in full DMEM medium. No sign of mycoplasma contamination was found for all cell lines. Cell line authentication was conducted using short tandem repeat profiling.

4.4. Plasmids, lentiviral vectors, and stable cell lines

Design of short hairpin RNA (shRNA#1 CCGGAAGGTGGGAGCCAGTAATTATCTCGAGATAATTACTGGCTCCCACCTTTTTTTG, shRNA#2 CCGGAACGCATCTTACCACATACAGCTCGAGCTGTATGTGGTAAGATGCGTTTTTTTG) targeting FBXO22 was used to knock down FBXO22 expression. DNA fragments (shRNA#1, shRNA#2) were inserted into the lentiviral vector pLKO.1 puro (Addgene, 10878). Plasmid transfection was performed as follows: 293 T cells were cultured in a 10 cm dish. When the confluency reached 30 %-40 %, the medium was replaced with serum-free DMEM, and co-transfection was carried out using transfection reagent EZ (20 μl, life-ilab, AC04L092) along with the target plasmid (5 μg) and packaging plasmids pMD2.G (5 μg, Addgene, 12259) and psPAX2(10 μg, Addgene, 12260). After 8-h transfection, the culture medium was replaced with full DMEM, and the cells were allowed to incubate for an additional 48–72 h. The supernatant containing lentivirus was collected, filtered through a 0.45 μm filter (PALL, 4614), and used for cell infection. The lentivirus-containing supernatant was mixed 1:1 with full DMEM medium. After infecting Re-HCS2/8 or Re-SW1353 cells for 48 h, cells were cultured in full DMEM medium containing puromycin (2 μg/ml,

BasalMedia, S250J0) for 24 h. The effectiveness of knockdown was validated using qRT-PCR and Western blot analysis.

4.5. FBXO22 siRNA transfection

FBXO22 siRNA transfection was performed by referring to the method described by Guo et al. for FBXO22 siRNA transfection [41]. Specific small interfering RNA (siRNA) targeting FBXO22 (siFBXO22, 5′-GGUGGGAGCCAGUAAUUAUTT-3′) as well as a non-specific control (siN, 5′-UUCUCCGAACGUGUCACGUTT-3′) were acquired from Tsingke (Shanghai, China). These siRNAs were transfected into CHS cells using Lipo8000™ Transfection Reagent (Beyotime, C0533) when the cells reached a confluency of 30–50 %. Approximately 6 h post-transfection, the medium containing transfection reagents was exchanged with full DMEM medium. After 48-h cell culture, qRT-PCR and WB analysis were performed to confirm that FBXO22 was down-regulated.

4.6. Western blot analysis and antibodies

Protein extracts underwent SDS-PAGE separation and subsequent transfer onto a nitrocellulose membrane (PALL, 66485), which was then blocked by 5 % skimmed milk in PBS and sequentially incubated with the indicated primary and secondary antibody using Odyssey CLx System and Image Studio (LI-COR Biosciences). Cropping of images from the original, unprocessed images was performed using Microsoft PowerPoint 2021 and Adobe Photoshop CC 2018.

The following primary antibodies were utilized in this procedure: rabbit Polyclonal antibody FBXO22 (1 μg/ml, Proteintech Group, 13606–1-AP), rabbit Polyclonal antibody PD-L1/CD274 (1.4 μg/ml, Proteintech Group, 17952–1-AP), rabbit Polyclonal antibody CDK5 (1.8 μg/ml, Proteintech Group, 10430-1-AP), and rabbit Polyclonal antibody GAPDH (0.12 μg/ml, Proteintech Group, 10494–1-AP).

4.7. qRT-PCR analysis

Total RNA was extracted in accordance with the manufacturer's instructions using Trizol (TAKARA, 108–95-2). Subsequently, the RNA was reverse transcribed into cDNA using HiScriptII Reverse Transcriptase (Vazyme, R222-01). This was followed by qRT-PCR utilizing the SYBR Green PCR Master Mix (Vazyme, Q711-02). The specific primers employed in the qRT-PCR are provided in Supplementary Table 1.

4.8. Colony formation assay

Colony formation assay was conducted by seeding 5000 cells/well for Re-HCS2/8 shN, Re-HCS2/8 shFBXO22 #2, Re-SW1353 shN or Re-SW1353 shFBXO22 #1. These cells were plated in six-well plates, and the culture medium was replaced every 2 days. After 1 weeks, the plates were stained with 1 % crystal violet (Sigma, C3886) and photographed. The analysis of the colonies was carried out using ImageJ (National Institutes of Health). Each experiment was repeated three times.

4.9. Cell proliferation assay

Using the Cell Counting Kit-8 (CCK8) assay (Beyotime Biotechnology, C0039), 5×10^3 cells were initially seeded into 96-well plates and allowed to incubate for 4 days, during which the culture medium was replaced every 2 days. Following the incubation, CCK8 solution was added to the wells of the plates and allowed to incubate for 1 h. The optical density (OD) value at 450 nm (Elx 800; BioTek Instruments) was then measured.

4.10. Wound healing assay

CHS cells were plated in 6-well culture plates and grown to 90 % confluence. Wounds were created using a 1000 μl micropipette tip. Cultures were rinsed with PBS and replaced with FBS-free DMEM, following which the cells were incubated at 37 °C for 24 h. Photographs were taken at 0 and 24 h and the area of the scratch was measured by Image J. Calculated cell migration rate= (0 h area − 24 h area)/0h area × 100 %.

4.11. Flow cytometry

Flow cytometry was performed using Annexin V-APC/PI Apoptosis Kit (Elabscience, E-CK-A217) according to the manufacturer's instructions. After digestion, cells were adjusted to a density of 1×10^5 cells/mL with Annexin V Binding Buffer, and incubated with Annexin V-APC Reagent and propidium iodide Reagent staining in the dark at room temperature for 15 min. After incubation, cells were diluted with Annexin V Binding Buffer and analyzed with a flow cytometer (BD Bioscience).

4.12. Immunohistochemistry

After immobilizing tumor tissue in 4 % paraformaldehyde for 24–48 h, tissues were embedded in paraffin, and cut into 4 μm sections. For IHC staining, these paraffin embedded tissue sections were deparaffinized, rehydrated, and subjected to heat-mediated antigen retrieval. After natural cooling, a 3 % hydrogen peroxide solution was applied to deactivate endogenous peroxidase for approximately 10 min. Following this step, the slides were washed three times with PBS. Subsequently, they were blocked with 5 % bovine serum albumin (BSA) at room temperature for a period of 30 min. The sections were immunostained with FBXO22(1:200, Proteintech Group, 13606–1-AP) or PD-L1/CD274 (1:300, Proteintech Group, 17952–1-AP) primary antibody and incubated at 4℃ overnight. On the second day, the slides were subjected to three 5-minute washes with PBS. Following this, they were incubated with the corresponding secondary antibody at room temperature for 1 h. After another three washes with PBS, the following steps were carried out: diaminobenzidine (DAB) staining, hematoxylin staining, dehydration using a gradient of ethanol, and finally, transparency achieved by submersion in xylene.

4.13. Statistical analysis

As outlined in the figure legends, statistical analyses were conducted employing the Student's *t*-test or Mann-Whitney *U* test. A significance level of $P < 0.05$ was used to determine statistical significance. The experiments were independently replicated a minimum of three times, consistently yielding similar results. The statistical analysis and figure generation were conducted using Prism 8.0 software (GraphPad Software) and SPSS version 25.0 (IBM). The data presented in the figures represent the average of three independent experiments and are expressed as the mean ± standard deviation (SD). Abbreviation: NS indicates not significant; *$p < 0.05$; **$p < 0.01$; ***$p < 0.001$; ****$p < 0.0001$.

Funding

The research plan was approved by the ethics committee, the experiment was conducted with relevant guidelines and regulations. The manuscript submitted does not contain information about medical device(s)/drugs. This work was supported by National Natural Science Foundation of China (8217277) and Shanghai Municipal Health and Family Planning Commission (201840209). No relevant financial activities outside the submitted work. We declare that we have no conflict of interest.

CRediT authorship contribution statement

Baoquan Xin: Writing – original draft, Methodology, Investigation,

Formal analysis, Data curation, Conceptualization. **Hui Chen:** Writing – original draft, Validation, Methodology, Investigation, Data curation, Conceptualization. **Zhi Zhu:** Visualization, Validation, Resources, Methodology, Investigation, Formal analysis. **Qiujing Guan:** Visualization, Validation, Methodology, Investigation, Formal analysis, Data curation. **Guangjian Bai:** Visualization, Methodology, Investigation. **Cheng Yang:** Validation, Resources, Methodology, Funding acquisition. **WeiWei Zou:** Visualization, Supervision, Resources, Methodology. **Xin Gao:** Validation, Supervision, Resources, Project administration, Formal analysis, Data curation, Conceptualization. **Lei Li:** Writing – review & editing, Supervision, Resources, Methodology, Investigation, Formal analysis, Data curation, Conceptualization. **Tielong Liu:** Writing – review & editing, Supervision, Resources, Methodology, Investigation, Funding acquisition, Formal analysis, Data curation, Conceptualization.

Declaration of competing interest

The authors declare the following financial interests/personal relationships which may be considered as potential competing interests: Tielong Liu reports financial support was provided by National Natural Science Foundation of China. Cheng Yang reports financial support was provided by Shanghai Municipal Health Commission. If there are other authors, they declare that they have no known competing financial interests or personal relationships that could have appeared to influence the work reported in this paper.

Appendix A. Supplementary data

Supplementary data to this article can be found online at https://doi.org/10.1016/j.jbo.2024.100605.

References

[1] H. Gelderblom, et al., The clinical approach towards chondrosarcoma, Oncologist 13 (2008) 320–329.
[2] R.F. Riedel, et al., The clinical management of chondrosarcoma, Curr. Treat. Options Oncol. 10 (2009) 94–106.
[3] J. Bruns, M. Elbracht, O. Niggemeyer, Chondrosarcoma of bone: an oncological and functional follow-up study, Ann. Oncol. 12 (2001) 859–864.
[4] N.G. Sanerkin, The diagnosis and grading of chondrosarcoma of bone: a combined cytologic and histologic approach, Cancer 45 (1980) 582–594.
[5] F.Y. Lee, et al., Chondrosarcoma of bone: an assessment of outcome, J. Bone Joint Surg. Am. 81 (1999) 326–338.
[6] F. Fiorenza, et al., Risk factors for survival and local control in chondrosarcoma of bone, J. Bone Joint Surg. Br. 84 (2002) 93–99.
[7] J.V. Bovée, L.J. van Den Broek, A.M. Cleton-Jansen, P.C. Hogendoorn, Chondrosarcoma is not characterized by detectable telomerase activity, J. Pathol. 193 (2001) 354–360.
[8] A.Y. Giuffrida, et al., Chondrosarcoma in the United States (1973 to 2003): an analysis of 2890 cases from the SEER database, J. Bone Joint Surg. Am. 91 (2009) 1063–1072.
[9] A. van Maldegem, et al., Outcome of first-line systemic treatment for unresectable conventional, dedifferentiated, mesenchymal, and clear cell chondrosarcoma, Oncologist 24 (2019) 110–116.
[10] L. Horn, et al., First-line atezolizumab plus chemotherapy in extensive-stage small-cell lung cancer, N. Engl. J. Med. 379 (2018) 2220–2229.
[11] C.H. June, R.S. O'Connor, O.U. Kawalekar, S. Ghassemi, M.C. Milone, CAR T cell immunotherapy for human cancer, Science 359 (2018) 1361–1365.
[12] P. Sharma, et al., Nivolumab in metastatic urothelial carcinoma after platinum therapy (CheckMate 275): a multicentre, single-arm, phase 2 trial, Lancet Oncol. 18 (2017) 312–322.
[13] H.A. Tawbi, et al., Pembrolizumab in advanced soft-tissue sarcoma and bone sarcoma (SARC028): a multicentre, two-cohort, single-arm, open-label, phase 2 trial, Lancet Oncol. 18 (2017) 1493–1501.
[14] L. Paoluzzi, et al., Response to anti-PD1 therapy with nivolumab in metastatic sarcomas, Clin Sarcoma Res 6 (2016) 24.
[15] M.J. Wagner, et al., Response to PD1 inhibition in conventional chondrosarcoma, J. Immunother. Cancer 6 (2018) 94.
[16] L. Zhang, et al., FBXO22 promotes the development of hepatocellular carcinoma by regulating the ubiquitination and degradation of p21, J. Exp. Clin. Cancer Res. 38 (2019) 101.
[17] M.K. Ge, et al., FBXO22 degrades nuclear PTEN to promote tumorigenesis, Nat. Commun. 11 (2020) 1720.
[18] R. Sun, et al., FBXO22 possesses both protumorigenic and antimetastatic roles in breast cancer progression, Cancer Res. 78 (2018) 5274–5286.
[19] X.N. Zhu, et al., FBXO22 mediates polyubiquitination and inactivation of LKB1 to promote lung cancer cell growth, Cell Death Dis. 10 (2019) 486.
[20] S. Chen, et al., Pan-cancer analyses reveal oncogenic role and prognostic value of F-box only protein 22, Front. Oncol. 11 (2021) 790912.
[21] C. Sun, R. Mezzadra, T.N. Schumacher, Regulation and function of the PD-L1 checkpoint, Immunity 48 (2018) 434–452.
[22] S. De, E.G. Holvey-Bates, K. Mahen, B. Willard, G.R. Stark, The ubiquitin E3 ligase FBXO22 degrades PD-L1 and sensitizes cancer cells to DNA damage, PNAS 118 (2021).
[23] L. Zhu, et al., A photoactivated Ru (II) polypyridine complex induced oncotic necrosis of A549 cells by activating oxidative phosphorylation and inhibiting DNA synthesis as revealed by quantitative proteomics, Int. J. Mol. Sci. 24 (2023) 7756.
[24] C. Schoen, et al., A potential osteogenic role for microRNA-181a-5p during palatogenesis, Eur. J. Orthod. 45 (2023) 575–583.
[25] S.C. Ferrante, et al., Adipocyte-derived exosomal miRNAs: a novel mechanism for obesity-related disease, Pediatr. Res. 77 (2015) 447–454.
[26] C. Xu, et al., CD147 monoclonal antibody attenuates abdominal aortic aneurysm formation in angiotensin II-Infused apoE-/-mice, Int. Immunopharmacol. 122 (2023) 110526.
[27] S. Dong, et al., Mechanisms of CCl4-induced liver fibrosis with combined transcriptomic and proteomic analysis, J. Toxicol. Sci. 41 (2016) 561–572.
[28] R.H. Khattab, et al., Multi-omics analysis of fecal samples in colorectal cancer Egyptians patients: a pilot study, BMC Microbiol. 23 (2023) 238.
[29] T. Yue, et al., Serum metabolomic profiling in aging mice using liquid chromatography—mass spectrometry, Biomolecules 12 (2022) 1594.
[30] M.K. Tan, H.J. Lim, J.W. Harper, SCF(FBXO22) regulates histone H3 lysine 9 and 36 methylation levels by targeting histone demethylase KDM4A for ubiquitin-mediated proteasomal degradation, Mol. Cell Biol. 31 (2011) 3687–3699.
[31] Y. Johmura, et al., Fbxo22-mediated KDM4B degradation determines selective estrogen receptor modulator activity in breast cancer, J. Clin. Invest. 128 (2018) 5603–5619.
[32] X. Tian, et al., F-box protein FBXO22 mediates polyubiquitination and degradation of KLF4 to promote hepatocellular carcinoma progression, Oncotarget 6 (2015) 22767–22775.
[33] Y. Zheng, et al., Knockdown of FBXO22 inhibits melanoma cell migration, invasion and angiogenesis via the HIF-1α/VEGF pathway, Invest. New Drugs 38 (2020) 20–28.
[34] J. Cheng, et al., Emerging role of FBXO22 in carcinogenesis, Cell Death Discov 6 (2020) 66.
[35] B. Wu, et al., F-box protein FBXO22 mediates polyubiquitination and degradation of CD147 to reverse cisplatin resistance of tumor cells, Int. J. Mol. Sci. 18 (2017).
[36] F. Zhang, et al., Characterization of drug responses of mini patient-derived xenografts in mice for predicting cancer patient clinical therapeutic response, Cancer Commun. (Lond) 38 (2018) 60.
[37] Y. Xiao, et al., Comprehensive metabolomics expands precision medicine for triple-negative breast cancer, Cell Res. 32 (2022) 477–490.
[38] C. Li, et al., Integrated omics of metastatic colorectal cancer, Cancer Cell 38 (2020) 734–747.e739.
[39] R. Liu, et al., Paclitaxel-eluting polymer film reduces locoregional recurrence and improves survival in a recurrent sarcoma model: a novel investigational therapy, Ann. Surg. Oncol. 19 (2012) 199–206.
[40] Y. Liu, et al., An injectable superior depot of Telratolimod inhibits post-surgical tumor recurrence and distant metastases, Acta Biomater. 141 (2022) 132–139.
[41] F. Guo, et al., FBXO22 suppresses metastasis in human renal cell carcinoma via inhibiting MMP-9-mediated migration and invasion and VEGF-mediated angiogenesis, Int. J. Biol. Sci. 15 (2019) 647–656.